Colloid Polym Sci 277:680–686 (1999)

SHORT COMMUNICATION

A. Larsson

The size and shape of silica particles

Received: 2 December 1998
Accepted in revised form: 2 February 1999

A. Larsson
Göteborg University
Department of Chemistry
Physical Chemistry
S-41296 Göteborg, Sweden
e-mail: zoombie@phc.chalmers.se
Tel.: +46-31-7722748 Fax: +46-31-167194

Abstract Negatively charged silica particles were investigated at pH 10.0. They were found to be rod-shaped (cylinder) with a diameter of 5–5.5 nm and a full length of 44–67 nm depending on the rod model used. Moreover, the particles were found to be stable against aggregation in the region 0.4–50 mM NaCl.

Key words Silica – Rod – Small angle scattering – Light scattering

Introduction

The asymmetry of nanosized colloidal particles can be evaluated by a number of methods. Young et al. [1] developed a method based on combining time-averaged light scattering (TLS) and dynamic light scattering (DLS). Rowell [2] proposed that the polarisation ratio between the vertical and horizontal component in a light scattering apparatus could be used to obtain the shape. Biddle et al. [3] developed a method based on combining capillary viscometry and DLS. Small-angle X-ray scattering (SAXS) [4] and small-angle neutron scattering [5] are other useful means of obtaining the size and shape of colloidal particles. The full potential of these methods is probably not yet recognised.

Small silica particles with a diameter of 5 nm can aggregate in various ways depending on the conditions used. Thus, under basic conditions in the absence of salt the particles grow symmetrically maintaining a spherical shape [6]. In the presence of salt spherical particles aggregate to form clusters of particles and can form three-dimensional networks. Small aggregates have a tendency to be more or less linear.

These particles have considerable importance in paper manufacture and are used in retention aid systems with cationic polyacrylamide or cationic starch [7]. Extensive flocculation studies of these system have been reported [8–13]. Also the particles electrical properties have been investigated by means of electrokinetic sonic amplitude by Rasmusson and Wall [14]. The shape of the particles has been investigated by Biddle et al. [3]; however, they used very fresh, specially prepared, silica samples.

They found the particles to have a short axis diameter of 2.2 nm and a long axis of 7.2 nm. This was confirmed by transmission electron micrographs. The silica sample used in this study was stored for about 6 months and corresponded to the samples used in the flocculation studies. The particles were investigated by means of TLS, DLS and SAXS.

Experimental

Materials

The silica was kindly provided by Eka Chemicals. It has a surface area of about $500\ m^2\ g^{-1}$ according to the manufacturer. The surface area corresponds to a spherical particle radius of about 2.5 nm.

Sample preparation

The silica dispersion was used as received and was diluted to appropriate concentrations with double-distilled water. The silica

dispersions were filtered twice through a 0.22 μm Millipore filter. All glassware used after the filtering step was carefully cleaned with condensing acetone. The pH was found to be 10.0 in all silica dispersions. The concentration of silica varied from 2.5 to 10 g l^{-1}.

Time-averaged light scattering

TLS was performed on a fully computerised goniometer from Malvern Instruments, UK. The light source was an argon ion laser with vertically polarised incident light operating at 488 nm from Spectra physics. It was found that the dissymmetry ratio R_{60}/R_{120} was never higher than 1.05. This was taken as a criterion that the particles were Rayleigh scatterers, i.e., $r < \lambda_0/20$ where r is the particle radius and λ_0 the wavelength of the incident light. Therefore the TLS data were only measured at one angle, namely $\theta = 90°$. The data were plotted as a Rayleigh equation with an interaction term which is given by [15]

$$\frac{K_0 c}{R_{90}} = \frac{1}{M_p} + 2B_2 c \ , \tag{1}$$

where c is the concentration of particles, R_{90} is the Rayleigh ratio, M_p is the molecular weight of the particles and B_2 is the second virial coefficient. K_0 is the optical constant which is given by [15]

$$K_0 = \frac{9\pi^2 n_0^4}{\lambda_0^4 N_A \rho_p^2}\left(\frac{n_p^2 - n_0^2}{n_p^2 + 2n_0^2}\right)^2 \ , \tag{2}$$

where n_p is the refractive index of the particles, n_0 is the refractive index of the solvent, N_A is Avogadro's number and ρ_p is the density of the particles. The molecular weight of the anhydrous particles can be converted to the volume of the particles, V_p, via

$$V_p = \frac{M_p}{N_A \rho_p} \ . \tag{3}$$

The volume of the particle can easily be converted to a spherical radius, r, according to

$$r = \sqrt[3]{\frac{3V_p}{4\pi}} \ . \tag{4}$$

The refractive index of the particles was taken as 1.455 and that of the solvent as 1.337. The density of the particles was taken as 2.2 g cm^{-3}.

Dynamic light scattering

The concentration fluctuation of particles in solution is due to motion of the centres of mass. This will give rise to fluctuations in the scattered light when light is shining through the solution. The function of interest in DLS is the field time-correlation function (TCF) which is given by [16]

$$g_1(t) = \frac{|\langle E^*(0)E(t)\rangle|}{|\langle E^*(0)E(0)\rangle|} \ , \tag{5}$$

where E is the amplitude of the electromagnetic field. The function is obtained from the experimentally directly accessible scattering intensity via the relationship [16]

$$\langle I(0)I(t)\rangle = G_2(t) = A + Bg_1^2(t) \ , \tag{6}$$

where A and B are time-independent constants and t is the delay time. The correlation function $G_2(t)$ is normalised with the correlation function at infinite time, i.e. [17],

$$G_2^0(t) = \frac{G_2(t)}{G_2(\infty)} = \frac{\langle I(0)I(t)\rangle}{\langle I\rangle^2} \ . \tag{7}$$

For homogenous monodisperse spherical particles this equation can be written as [17]

$$G_2^0(t) = \langle I\rangle^2(1 + Ce^{-\Gamma t}) \ , \tag{8}$$

where C is the efficiency of the detector. Thus, the TCF decays with a single exponential decay where the diffusion coefficient, D, of the particles is given by [16, 17]

$$\Gamma = Dq^2 \ . \tag{9}$$

The diffusion coefficient is related to the hydrodynamic radius for spherical particles by [16, 17]

$$r_h = \frac{k_B T}{6\pi\eta D} \ , \tag{10}$$

where r_h is the hydrodynamic radius, k_B is Boltzmann's constant, T is the absolute temperature and η is the viscosity of the solvent.

The DLS measurements were performed on the same apparatus as the TLS measurements at an angle of 90°. The data could be fitted with a single exponential decay.

Small-angle X-ray scattering

X-rays interact with the electrons of an atom and the intensity of scattered radiation is given by [18]

$$I(q) = AN_p V_p^2(\rho_p - \rho_m)^2 P(q) \ , \tag{11}$$

where A is a calibration constant, N_p the number of particles, V_p the volume of the particles, and ρ_p and ρ_m are the scattering length density of particles and medium, respectively. $P(q)$ is as usual the form factor. The scattering vector q can, as usual, be derived via the equation [19]

$$q = \frac{4\pi}{\lambda}\sin(\theta/2) \ , \tag{12}$$

where λ is the wavelength of the incident radiation and θ is the scattering angle. The scattering length density is correlated to the scattering length b via the relation [19]

$$\rho = \frac{b}{V} \ , \tag{13}$$

where V is the volume of particles or the volume of the medium molecules. The scattering length can be calculated from [19], namely,

$$b = b_0 z \ , \tag{14}$$

where $b_0 = 0.282 \times 10^{-12}$ cm and z is the number of electrons in the molecule; however, at larger scattering angles, θ, the full Thomson formula [20]

$$b_0 = \left(\frac{1 + \cos^2\theta}{2}\right)0.282 \times 10^{-12} \tag{15}$$

must be used.

SAXS measurements were performed at the Synchrotron Radiation Source at Daresbury Laboratories, UK using the beamline NCD 8.2. The q range covered in these experiments was 0.025–2.5 nm^{-1}. The q range was derived from two different camera lengths (4.5 m and 0.6 m yielded scattering vectors $0.025 \le q_1 \le 0.5$ nm^{-1} and $0.1 \le q_2 \le 2.5$ nm^{-1}, respectively.) An absolute q calibration was obtained through subtraction of parasitic (slits) and background scattering (water solution and mylar window material) using the procedure introduced by Vonk [21]. Since the shape of the particles was under investigation the apparatus was not calibrated to an absolute scale of intensity. The form factor can be obtained for noninteracting particles via the formula [15]

$$P(q) = I(q)/I_0 \ . \tag{16}$$

This is also a good approximation as long as $2B_2M_pc << 1$; however, calculations show that the interaction term cannot be neglected. In this case Eq. (16) must be rewritten to account for particle interactions according to [15]

$$I(q) = AN_pV_p^2(\rho_p - \rho_m)^2P(q)S(q) \ , \tag{17}$$

where $S(q)$ is the structure factor. The structure factor is related to the radial distribution function $g(r)$ via the relation [15]

$$S(q) = 1 + \frac{4\pi\rho_0}{q}\int_0^\infty r[g(r) - 1]\sin(qr)\,dr \ , \tag{18}$$

where ρ_0 is the average density of particles. Using the mean spherical approximation as given by Hayter and Penfold [22] the $S(q)$ value based on the electrostatic repulsive potential can be calculated. It was found that under the experimental conditions used $S(q) = 1$, i.e., particle interactions do not affect the form factor $P(q)$.

Results and discussion

Time-averaged light scattering

The TLS data of the silica particles given by Eq. (1) are shown in Fig. 1. They are plotted as K_0c/R_{90} versus c. It can be seen that at zero concentration all data converge to the same value at the y-axis. This value corresponds to $1/M_p$ and gives the molecular weight of the particles. It was found to be $2.16 \pm 0.10 \times 10^6\,g\,mol^{-1}$. It corresponds to a spherical radius of 7.3 ± 0.1 nm. Furthermore, since the data converge to one value irrespective of the electrolyte concentration this indicates that the particles do not aggregate between 0.4 and 50 mM NaCl. The second virial coefficients extracted from Fig. 1 are summarised in Table 1. The second virial coefficient decreases as the electrolyte content increases.

Dynamic light scattering

The DLS data could be fitted by a single exponential decay which gave a diffusion coefficient of $2.55 \pm 0.10 \times 10^{-7}\,cm^2\,s^{-1}$. This corresponds to a hydrodynamic radius of 9.6 ± 0.4 nm. These data are rather approximate but indicate that the particles are too small to be evaluated by the combination of TLS and DLS at an incident wavelength of 488 nm. Therefore the shape of the particles was evaluated by SAXS.

Small-angle X-ray scattering

The scattering curve obtained for 0.5% wt and 1.0% wt silica indicated that the particles were rod-shaped. Three procedures were utilised in order to obtain the radius of the rod and the full length. In Fig. 2 the form factor $P(q)$ is plotted versus the

Table 1 The second virial coefficient, B_2, as a function of electrolyte concentration: it decreases as the electrolyte concentration increases

NaCl concentration (mM)	B_2 (mol cm^3 g^{-2})
0.4	3.84×10^{-5}
2	1.83×10^{-5}
10	8.25×10^{-6}
50	4.95×10^{-6}

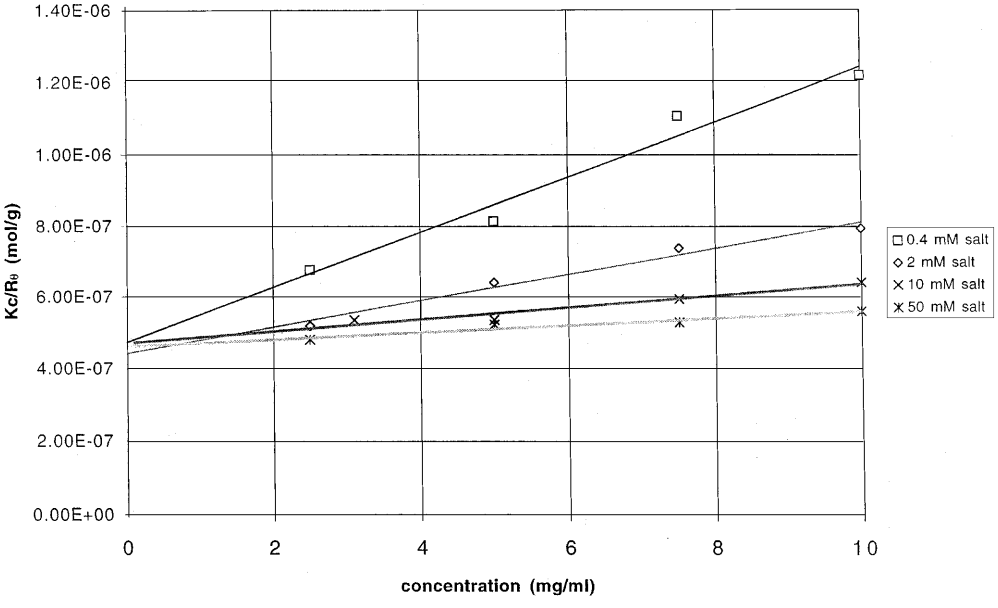

Fig. 1 Light scattering data of the silica particles. They are plotted as K_0c/R_θ versus c. It can be seen that, within experimental error, the data converge to the same value at the y-axis. This value corresponds to $1/M_p$. The molecular weight of the particles was found to be 2.16×10^6 g mol^{-1}. This corresponds to a spherical radius of 7.3 nm. The second virial coefficients as a function of electrolyte concentration are given in Table 1

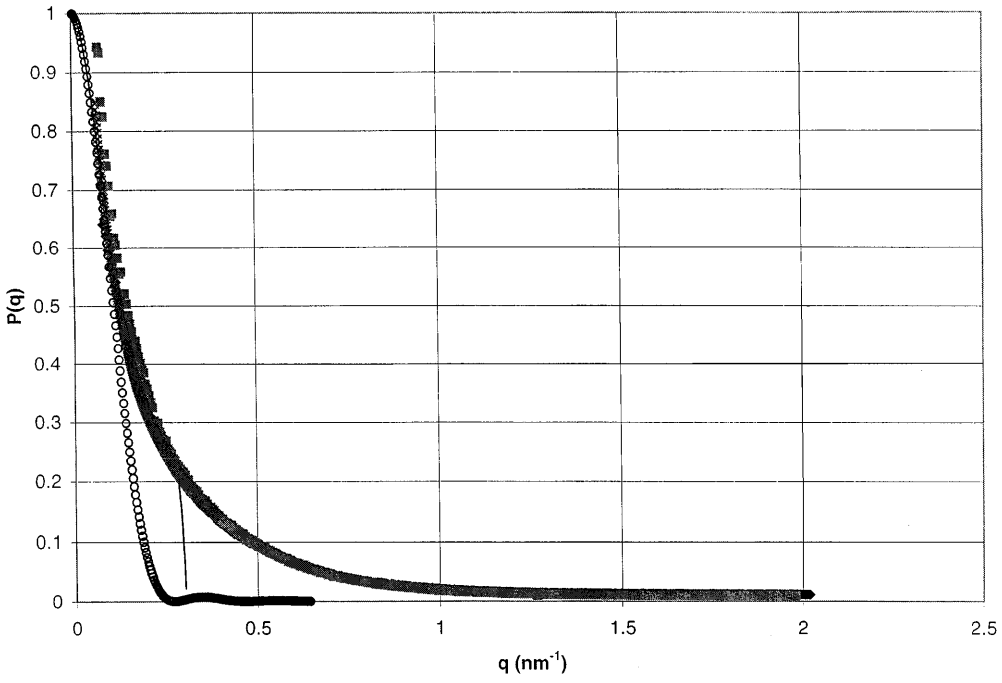

Fig. 2 Small-angle X-ray scattering (*SAXS*) data of the silica particles, ◆ and ■ 0.5 NSP. They are plotted as the form factor $P(q)$ versus the scattering vector q. Within experimental error the scattering data contain no structure. The data were fitted with the thin rod model. The thin rod model was further expanded (Eq. 20) to obtain a radius. This is shown as ×, in the figure. This full length of the rod was found to be 44 nm and the radius was found to be 2.5 nm. The background scattering at high q values has not been fitted. For comparison the scattering curve of a sphere (○) of the same radius of gyration, i.e., 12.8 nm is given. This corresponds to a spherical radius of 16.5 nm

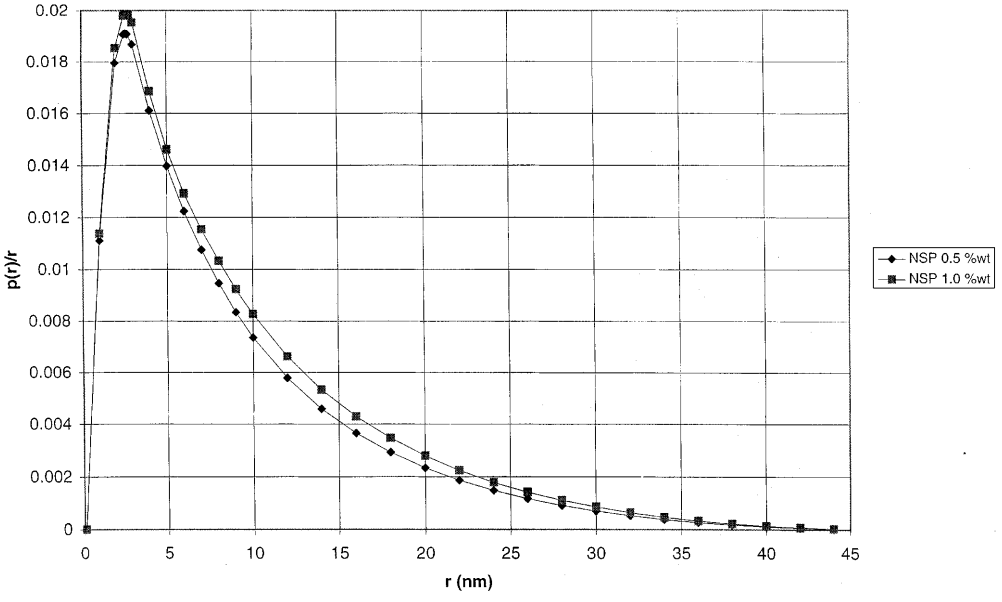

Fig. 3 SAXS data Fourier transformed to real space. The distance distribution function $p(r)$ is plotted as $p(r)/r$ against r. The radius of the cylinder is 2.7 nm and the full length is 44 nm

scattering vector q. The scattering curves of 0.5%wt and 1.0%wt silica have been normalised in order to check whether the structure factor $S(q)$ will affect the scattering curve or not: the form factor is not affected by any structure in the system. The data can now be fitted with an infinitesimally thin rod, i.e., it has no radius. The form factor is given by [23]

$$P(q) = \frac{2}{X}\left(\int_0^x \frac{\sin t}{t}\,\mathrm{d}t\right) - \left(\frac{\sin X/2}{X/2}\right)^2, \tag{19}$$

where $X = lq$ and l is the full rod length. The integral can be expanded by the function

$$\int_0^x \frac{\sin t}{t}\,\mathrm{d}t \cong X - \frac{X^3}{3{*}3!} + \frac{X^5}{5*5!} - \frac{X^7}{7*7!} + \frac{X^9}{9*9!} - \cdots. \tag{20}$$

Fourteen terms were included in this expansion. Fitting the data at small q gives the full length of the particles. Furthermore expanding the thin rod equation in order to obtain a radius, a, of the rod gives [24]

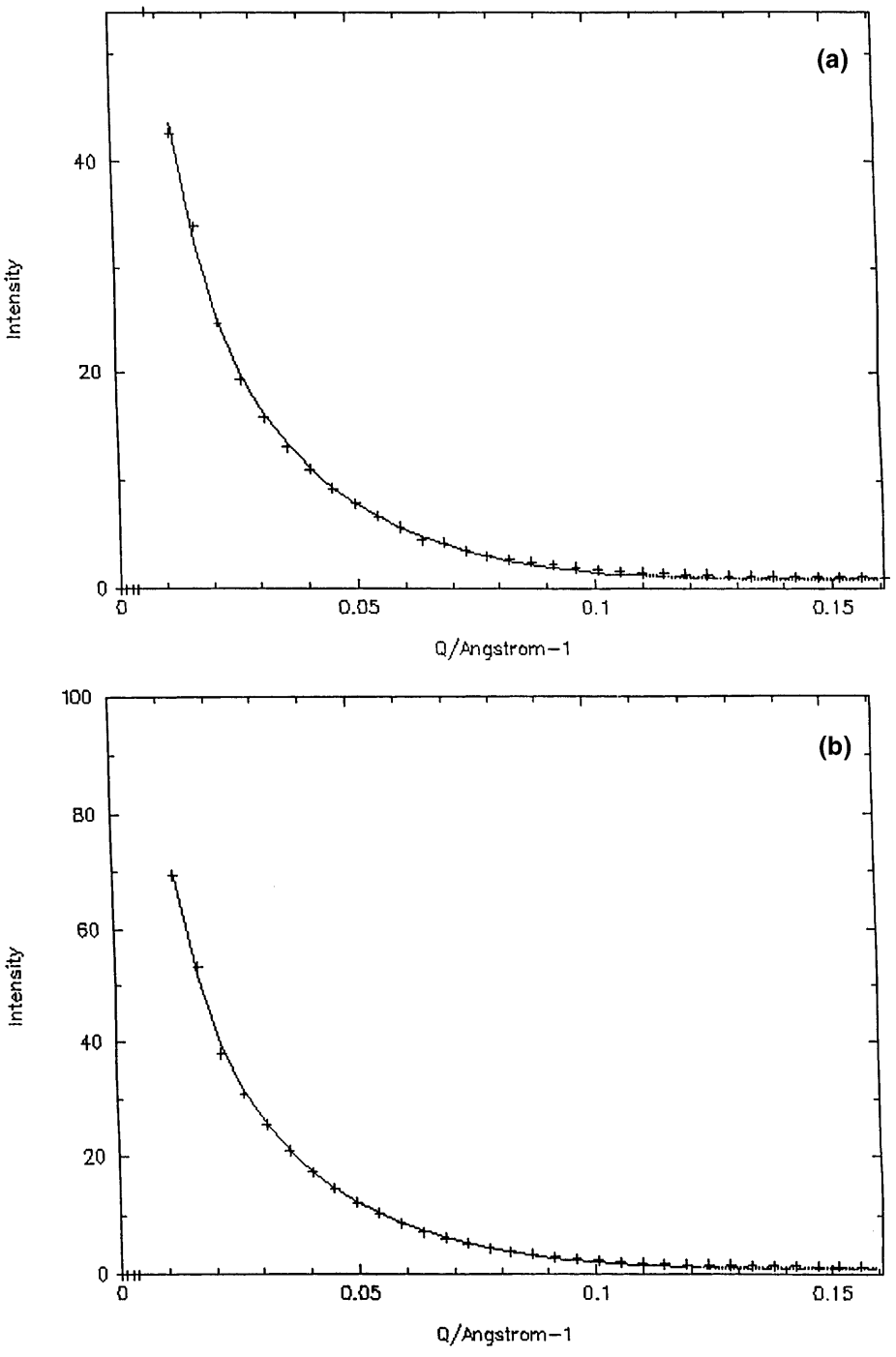

Fig. 4a, b SAXS data where the intensity (a.u.) is given as a function of the scattering vector q. In **a** the data are for 0.5% wt silica fitted by Eq. (24). In **b** the data are fitted for 1.0% wt silica. The result was the same in both cases. The radius is 2.5 nm and the full length is 67 nm

$$P(q) = \left(\frac{\pi}{qL} - \frac{2}{(qL)^2}\right)\left(1 - \frac{q^2a^2}{5}\right) \quad . \tag{21}$$

The procedure used is to place a sphere at each scattering point on the rod; the expansion is only valid when $qa < 1$ and $qL > 1$. Fitting the curve at slightly higher q values gives the rod radius. By this procedure the radius of the cylinder was found to be 2.5 nm and the full length 44 nm. For comparison the scattering curve of a sphere of the same radius of gyration is plotted. It is apparent from this plot that the particles are rod-shaped.

The data can also be converted to real space via a direct Fourier transform according to the following equation [4, 25]:

$$\gamma(r) = \frac{1}{2\pi^2}\int_0^\infty I(q)q^2\frac{\sin qr}{qr}\mathrm{d}q \ . \quad (22)$$

The characteristic function, $\gamma(r)$, is related to the distance distribution function by [26, 27]

$$p(r) = 4\pi r^2\gamma(r) \ . \quad (23)$$

The distance distribution function represents the system's behaviour in real space. Glatter [28] pointed out that the function $p(r)/r$ is a more sensitive indication of shape than $p(r)$. Comparison of these results with the calculations of Glatter [28] shows them to be strongly indicative of homogenous cylinders. The radius of the rod can be obtained from the maximum in the curve shown in Fig. 3 and the full length can be obtained from the curve where $p(r)/r$ goes to zero. The radius of the cylinder was found to be 2.7 ± 0.2 nm and the full length 44 nm.

A third method to obtain the radius of the rod and the full length is via the equation [25, 29]

$$p(q) = \int_0^{\pi/2}\frac{\sin^2(qH\cos\beta)}{q^2H^2\cos^2\beta}\frac{4J_1^2(qR\sin\beta)}{q^2R^2\sin^2\beta}\sin\beta\ \mathrm{d}\beta, \quad (24)$$

where the height of the cylinder (full length) is $2H$ and R is the radius. β is the angle between the axis of the cylinder and the bisectric. $J_1(qR\sin\beta)$ is a Bessel function of order 1. For computational purposes the data were fitted with a program developed at ILL called cdisc using a least-squares fitting routine called fitfun developed by Ghosh [30]. The fit is shown in Fig. 4. The radius of the cylinder was found to be 2.5 nm and the full length 67.2 nm.

The data of the fits are summarised in Table 2. Clearly, the particles are rod-shaped and the radius of the rod was found to be 2.5 nm; however, the full length of the rod varies in the different procedures probably due to different weighings used in the models. It must be emphasised that particles made under more controlled circumstances, i.e., in a laboratory experiment were also rod-shaped [3].

Table 2 The radius of the rod and the full length calculated according to the different procedures outlined in the text

Model	Equations	Radius (nm)	Full length (nm)
Thin rod	19–21	2.5	44
Fourier transformation	22–23	2.7	44
Rod	24	2.5	67

The radius of gyration of a rod is given by [25]

$$r_g^2 = \frac{r^2}{2} + \frac{l^2}{12} \quad (25)$$

and for a sphere by [25]

$$r_g^2 = \frac{3r^2}{5} \ . \quad (26)$$

We can therefore compare the radius of gyration obtained with TLS and SAXS. The radius of gyration of the TLS data as calculated from the spherical particle radius is 5.7 nm. The radii of gyration calculated for the different rod models obtained from SAXS are 12.8 nm and 19.5 nm, respectively: the particles are small. As TLS measurements were made at only one angle and an effective solid radius was calculated from the total intensity, it is not unreasonable for there to be a substantial discrepancy compared to SAXS data. The usual Guinier plot to obtain the radius of gyration at small scattering vectors could not be applied in the SAXS measurements as no linear region was found. The intensity increases rapidly as the scattering vector q decreases in the low q region. It must be emphasised that even if the radius of gyration was obtained in an approximate way the data are still in good agreement.

Acknowledgements R.H. Ottewill is gratefully acknowledged for the use of the light scattering apparatus. He is also acknowledged for help in the calculations of the cylinder using the cdisc program. Peter-Paul van de Moor is gratefully acknowledged for using part of his beamtime at Daresbury and for making the necessary background correction. Eka Chemicals is thanked for financial support.

References

1. Young CY, Missel PJ, Mazer NA, Benedek GB, Carey MC (1978) J Phys chem 82:1375
2. Rowell RL (1990) In: Candau F, Ottewill RH (eds) An introduction to polymer colloids. Kluwer, Norwell, p 196
3. Biddle D, Walldal C, Wall S (1996) Colloids Surf A 122:169
4. Porod G (1951) Kolloid-Z 124:83
5. Nabavi M, Spalla O, Cabane B (1993) J Colloid Interface Sci 160:459
6. Iler RK (1979) In: The chemistry of silica. Wiley, New York, p 174
7. Andersson K, Lindgren E (1996) Nord Pulp Paper Res J 1:15
8. Walldal C, Wall S, Biddle D (1998) Colloids Surf A 131:203
9. Larsson A, Wall S (1998) Colloids Surf A 139:259
10. Larsson A (1998) Colloids Surf B 12:23
11. Larsson A, Rasmusson M (1997) Carbohydr Res 304:315
12. Dahlberg A, Larsson A, Åkerman B, Wall S (1999) Colloid Polym Sci (in press)
13. Larsson A, Walldal C, Wall S (1999) Colloids Surf A (submitted)
14. Rasmusson M, Wall S (1997) Colloids Surf A 122:169
15. Ottewill RH, Richardson RA (1982) Colloid Polym Sci 260:708
16. Burchard W, Richtering W (1989) Prog Colloid Polym Sci 80:151

17. Berne BJ, Pecora R (1975) In: Dynamic light scattering. Wiley, New York
18. Cabane B (1986) In: Zana R (ed) Surfactant solutions: new methods of investigation. Surfactant science series, vol 2. Dekker, New York, pp 57–145
19. Cotton JP (1991) In: Lindner P, Zemb T (eds) Neutron, X-ray and light scattering: introduction to an investigative tool for colloidal and polymeric systems. North Holland, Amsterdam, pp 3–18
20. Glatter O (1991) In: Lindner P, Zemb T (eds) Neutron, X-ray and light scattering: introduction to an investigative tool for colloidal and polymeric systems. North Holland, Amsterdam, pp 33–82
21. Vonk CG (1973) J Appl Crystallogr 6:81
22. Hayter JB, Penfold J (1981) Mol Phys 42:109
23. Burchard W (1983) Adv Polym Sci 48:1
24. Higgins JS, Benoit HC (1994) In: Polymers and neutron scattering. Clarendon Press, Oxford, pp 170–172
25. Burkitt SJ, Ottewill RH, Hayter JB, Ingram BT (1987) Colloid Polym Sci 265:619
26. Kratky O, Porod G (1948) Acta Phys Austriaca 2:133
27. Guinier A, Fournet G (1955) In: Small angle scattering of X-rays. Wiley, New York
28. Glatter O (1979) J Appl Crystallogr 12:166
29. van de Hulst HC (1981) In: Light scattering by small particles. Wiley, New York
30. Ghosh R (1989) In: FITFUN – an interactive/graphical fitting routine. ILL report 89GHO8T. Institute Laue Langevin, Grenoble